Journal of Zhejiang University-SCIENCE A (Applied Physics & Engineering)
ISSN 1673-565X (Print); ISSN 1862-1775 (Online)
www.zju.edu.cn/jzus; www.springerlink.com
E-mail: jzus@zju.edu.cn

# Microstructure and mechanical properties of liquid phase sintered silicon carbide composites

Jing-mei MA[†1], Feng YE[†‡1], Yan-ge CAO[2], Chun-feng LIU[1], Hai-jiao ZHANG[1]

([1]*School of Materials Science and Engineering, Harbin Institute of Technology, Harbin 150001, China*)

([2]*Air China Corporation Limited Engineering and Technology Branch, Beijing 101312, China*)

[†]E-mail: hgdmjm2006@yahoo.com.cn; yf306@hit.edu.cn

Received Apr. 13, 2010; Revision accepted June 28, 2010; Crosschecked Aug. 17, 2010

**Abstract:** Silicon carbide (SiC) composites were prepared by hot-press sintering from α-SiC starting powders with $BaAl_2Si_2O_8$ (BAS). The effects of additives on densification, microstructure, flexural strength, and fracture behavior of the liquid phase sintered (LPS) SiC composites were investigated. The results show that the served BAS effectively promotes the densification of SiC composites. The flexural strength and fracture toughness of the SiC composites can reach a maximum value of 454 MPa and 5.1 $MPa \cdot m^{1/2}$, respectively, for 40% (w/w) BAS/SiC composites. SiC grain pullout, crack deflection, and crack bridging were main toughening mechanisms for the sintered composites.

**Key words:** Silicon carbide (SiC), $BaAl_2Si_2O_8$ (BAS), Liquid phase sintered (LPS), Mechanical properties
**doi:**10.1631/jzus.A1000162 **Document code:** A **CLC number:** TG146.2

## 1 Introduction

Silicon carbide (SiC) ceramic is one of the most promising materials for engineering applications due to its high hardness, good chemical erosion resistance, good oxidation resistance, and excellent mechanical properties (Schwetz, 2000; Zhou *et al.*, 2001; Lee *et al.*, 2005; Magnani *et al.*, 2008; Hotta and Hojo, 2009). However, it is difficult to obtain full dense SiC ceramic with a traditional sintering method. In general, boron, carbon, or aluminium was used in solid-phase sintering for SiC. The sintering temperature of densify SiC ceramic in solid-state method was up to 2200 °C. In recent years, liquid-phase sintered SiC has been successfully developed with AlN, $Y_2O_3$, or simultaneous addition of $Y_2O_3$ and $Al_2O_3$ as sintering additives. $SiO_2$ derived from the surface oxide of SiC powders will react with these additives, resulting in liquid phases and facilitating densification at a lower sintering temperature (2000 °C) (Rixecker *et al.*, 2001; Choi *et al.*, 2002; Kim *et al.*, 2002; Baud *et al.*, 2003a; 2003b; Ihle *et al.*, 2005a; 2005b; 2005c; Suzuki and Sasaki, 2005). The liquid phases at the grain boundary, however, will soften and degrade the high-temperature properties of these composites. Therefore, it is necessary to investigate a good additive system with a high melting point, which subsequently crystallizes completely into a compound.

$BaAl_2Si_2O_8$ (BAS) is an advanced glass-ceramic with a high melting temperature of 1760 °C (Lee and Aswath, 2000; 2001; Bansal, 2003; Ye *et al.*, 2003; 2008; Liu *et al.*, 2009), which easily forms eutectic around 1175 °C. During the cooling process, BAS will readily crystallize into a refractory compound. Recent studies show that BAS glass-ceramic effectively promotes the densification of $Si_3N_4$ composites (Yu and White, 2001; Yu *et al.*, 2001; Chen *et al.*, 2002; Liu *et al.*, 2009; Ye *et al.*, 2010). Therefore, BAS is expected to be an effective liquid phase sintering aid for SiC densification.

The objective of the present work is to study the

‡ Corresponding author

effects of BAS content on the microstructure and mechanical properties of SiC composites sintered at a lower temperature (1800 °C). The toughening mechanisms are also discussed.

## 2 Experimental

The materials used in this study were α-SiC with different contents of BAS (20%–40%, w/w). The starting powders were α-SiC (Fig. 1), $BaCO_3$ (99.9% purity, Rare Metallic Co., Ltd., Japan), $Al_2O_3$ (Grade A16SG, Alcoa) and $SiO_2$ (99.9% purity, Rare Metallic Co., Ltd., Japan). The $BaCO_3$, $Al_2O_3$, and $SiO_2$ powders were mixed in a molar ratio of 1:1:2, resulting in BAS liquid phase during the sintering. When calculating the overall composites, $SiO_2$ on the surface of SiC powders was taken into account according to the manufacturer's specifications.

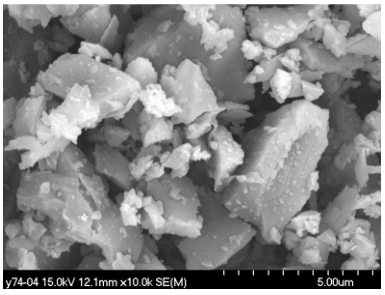


**Fig. 1 SEM micrograph of original α-SiC powders**

The three powder batches were blended simultaneously for 12 h by wet-milling with silicon nitride balls, using ethanol as the milling media. The dried blends were dispersed with 100 meshes by hand. Finally, the mixed powders were packed into a graphite die coated with boron nitride, and were hot-pressed at 1800 °C for 1 h in a 0.1 MPa nitrogen atmosphere under a pressure of 30 MPa.

The bulk densities of the sintered composites were measured by the Archimedes' principle. The phase compositions of the SiC composites were determined via X-ray diffractometry (XRD) (Model D/max-γB, Rigaku, Japan), using CuK$\alpha$ radiation. The diffraction data were collected over a $2\theta$ range of 10°–65°, with a step width of 0.02° and a scan rate of 4°/min. The generator settings were 40 kV and 200 mA.

The microstructures of the polished surfaces and fracture surfaces of the sintered composites were characterized by scanning electron microscope (SEM) equipped with energy-dispersive X-ray spectroscopy (EDX). Before observation, these samples were coated with a thin gold film to make the surface conductive.

The flexural strength and fracture toughness at room temperature were measured. For all flexural bars, the tensile surface lies perpendicular to the hot-pressing direction. 3 mm×4 mm×36 mm bar specimens were used for flexural strength measurements using a three-point bending fixture with a span of 30 mm. The elastic modulus of the composites was determined from the stress-strain curve recorded by attaching strain gauge to the tensile surface of specimen. Fracture toughness was measured by the single edge notch beam (SENB) method with a span of 16 mm using 2 mm×4 mm×20 mm bars. A half-thickness notch was made using a diamond wafering blade. At least six specimens were machined for fracture analyses.

## 3 Results and discussion

### 3.1 Phase composition and microstructure characterization

The densities of the SiC composites increase with the increase of BAS contents from 20%–40% (w/w), as shown in Table 1. It indicates that it is possible to obtain nearly full density BAS/SiC composites at a lower sintering temperature (1800 °C) by hot-press sintering.

**Table 1 Relative density and mechanical properties of BAS/SiC composites**

| Content of BAS (%, w/w) | Relative density (%) | Flexural strength (MPa) | Fracture toughness (MPa·m$^{1/2}$) | Young's modulus (GPa) |
|---|---|---|---|---|
| 20 | 86.6 | 199±3 | 2.9±0.2 | 164.6±1.5 |
| 30 | 93.8 | 312±19 | 4.7±0.4 | 229.7±1.6 |
| 40 | 95.8 | 454±5 | 5.1±0.6 | 264.2±0.9 |

Careful examination of the XRD results is summarized in Fig. 2. It clearly shows that all three sintered SiC composites are composed of α-SiC (6H) and hexagonal BAS phases. The presence of the 6H-SiC types can be established unambiguously from the isolated *hkl* peaks for the 6H polytype (Ortiz *et al.*, 2000). With respect to the hexagonal BAS phase, several well-defined peaks can be observed in the XRD patterns, revealing that hexacelsian was the

predominant crystalline phase in the BAS matrix. No other compounds were found which was attributed to the stoichiometric reaction among $BaCO_3$, $Al_2O_3$, and $SiO_2$ powders during the sintering process. There was also no celsian phase detected in these composites. This is due to the sluggish kinetics of hexacelsian to Celsian phase transformation (Bansal and Hyatt, 1989; Liu *et al.*, 2010).

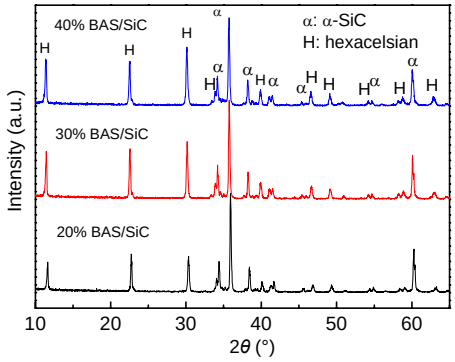


**Fig. 2 X-ray diffraction patterns of BAS/SiC composites**

Fig. 3 demonstrates the typical microstructure of the BAS/SiC composites with different BAS contents after 1800 °C sintering. It is easy to distinguish blackish SiC particles from the bright BAS phase according to the different atomic number. EDS analysis from the SEM images also confirms the above identification. SEM observations revealed that the SiC particle was oriented in the fine and continuous BAS phase. Fig. 3a shows clearly that there are holes in the 20% (w/w) BAS/SiC composites, which is consistent with the density test results (Table 1). This indicates that the sintering temperature in this study is slightly low for the 20% (w/w) BAS/SiC composites densification.

### 3.2 Mechanical properties

The flexural strengths of BAS/SiC composites at room temperature are shown in Table 1. It can be seen that the flexural strengths of the composites increase with increasing BAS contents. Although the thermal mismatch stress between the BAS matrix and SiC particles will destroy the strengthening effect, by further increasing the content of BAS to 40% (w/w), the strength of the composites increase ($\alpha_{\text{Hexacelsian}}=8\times10^{-6}$/°C, $\alpha_{\text{SiCp}}=4.5\times10^{-6}$/°C) (Ye *et al.*, 2001). The strength of the 40% (w/w) BAS/SiC composite increases 191% compared to the pure BAS matrix (156 MPa) (Ye *et al.*, 2001). This can be attributed to the good load transformation effect from BAS to SiC particles in the BAS/SiC composite and the higher (95.8% of the theoretical density) density induced by the higher hexacelsian phase contents.

Fracture toughness of the BAS/SiC composites at room temperature is illustrated in Table 1. The fracture toughness increases with the increase of BAS content. The fracture toughness of the composites with 30% and 40% (w/w) BAS reach 4.7 and 5.1 $MPa\cdot m^{1/2}$, respectively. The fracture toughness of 40% (w/w) BAS/SiC composite increases 264% compared with the pure glass-ceramic matrix (1.4 $MPa\cdot m^{1/2}$) reported by Ye *et al.* (2001). Fracture surfaces of the 30% and 40% (w/w) BAS/SiC composites after three-point bending tests are shown in Fig. 4. The fractural surfaces are quite rough, where the SiC particles pull-out and their residual holes can be seen. The fracture toughness of 40% (w/w) BAS/SiC composite is higher than that of 30% (w/w) BAS/SiC composite, which is ascribed to the high content of the BAS melt.

As shown in Table 1, with the increase of BAS

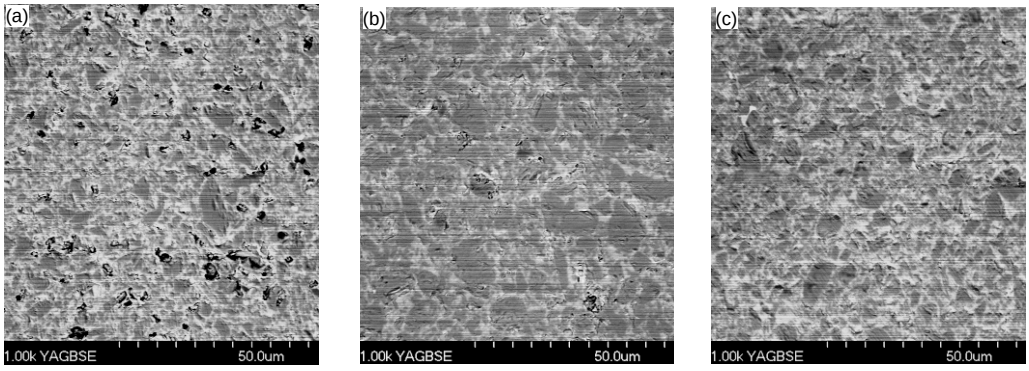


**Fig. 3 SEM micrographs of SiC/BAS composites with different contents of BAS (w/w). (a) 20% (b) 30% (c) 40%**

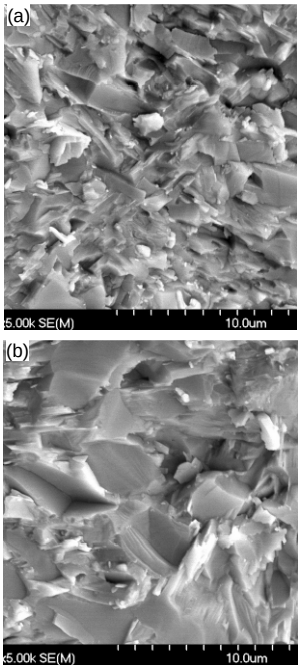


**Fig. 4 Fractographs of as-sintered 30% (w/w) BAS/SiC (a) and 40% (w/w) BAS/SiC composites (b)**

content, the Young's modulus of the BAS/SiC composites increases. This should relate to the relative density of the BAS/SiC composites. The technical process of the ceramics has an important effect on their Young's modulus. In general, the Young's modulus of composites containing pores can be estimated as

$$E / E_0 = 1 - kP,$$

where $E_0$ is the Young's modulus of the composite without porosity and $k$ is a constant. When the porosity $P$ is small, the Young's modulus of the composite will be linearly decreased with the increase of porosity (Zhang *et al.*, 2007).

The crack propagation produced by a Vickers indentation in the 30% (w/w) BAS/SiC composites is shown in Fig. 5. It can be seen that the propagation crack tends to deflect along the SiC particles and the BAS phase interface. SiC particles pull-out and crack bridging can also be seen in the wake of the extending cracks. This rough fracture path may explain the higher mechanical properties of the composites. Further increasing the sintering temperature of hot-pressing may be favorable to obtain nearly full density SiC-based composites, and subsequently improving the mechanical properties of BAS/SiC composites, which will be investigated in detail in future.

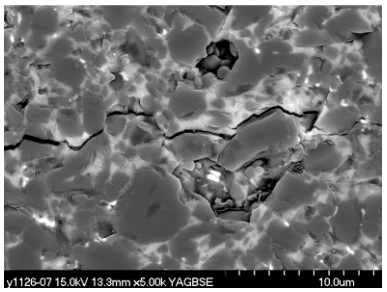


**Fig. 5 SEM micrograph of indentation crack paths in 30% (w/w) BAS/SiC composites showing crack deflection along SiC particles**

## 4 Conclusions

SiC ceramics with different contents (20%, 30%, and 40%) (w/w) of BAS were fabricated by a hot-pressing method at 1800 °C. The absence of $BaCO_3$, $Al_2O_3$, and $SiO_2$ in the final composites denoted complete crystallization of BAS during sintering. The relative densities and mechanical properties of the BAS/SiC composites increase with increasing BAS content. The mechanical properties depend strongly on the relative densities and SiC contents. The main toughening mechanisms are SiC pull-out, crack deflection, and bridging.

## References

Bansal, N.P., 2003. Celsian formation in fiber-reinforced barium aluminosilicate glass-ceramic matrix composites. *Materials Science and Engineering: A*, **342**(1-2):23-27. [doi:10.1016/S0921-5093(02)00313-1]

Bansal, N.P., Hyatt, M.J., 1989. Crystallization behavior and properties of $BaO{\cdot}Al_2O_3{\cdot}2SiO_2$. *Journal of Materials Research*, **4**(5):1257-1265. [doi:10.1557/JMR.1989.1257]

Baud, S., Thévenot, F., Chatillon, C., 2003a. High temperature sintering of SiC with oxide additives: IV. Powder beds and the influence of vaporization on the behaviour of SiC compacts. *Journal of the European Ceramic Society*, **23**(1):29-36. [doi:10.1016/S0955-2219(02)00070-5]

Baud, S., Thévenot, F., Pisch, A., Chatillon, C., 2003b. High temperature sintering of SiC with oxide additives: I. Analysis in the $SiC\text{-}Al_2O_3$ and $SiC\text{-}Al_2O_3\text{-}Y_2O_3$ systems. *Journal of the European Ceramic Society*, **23**(1):1-8. [doi:10.1016/S0955-2219(02)00067-5]

Chen, S., Ye, F., Zhou, Y., 2002. Low temperature hot-pressing BAS matrix composites reinforced with in situ

grown $Si_3N_4$ whiskers. *Ceramics International*, **28**(1): 51-58. [doi:10.1016/S0272-8842(01)00057-8]

Choi, H.J., Lee, J.G., Kim, Y.M., 2002. Oxidation behavior of liquid-phase sintered silicon carbide with aluminum nitride and rare-earth oxides ($Re_2O_3$, where Re=Y, Er, Yb). *Journal of the American Ceramic Society*, **85**(9):2281-2286. [doi:10.1111/j.1151-2916.2002.tb00448.x]

Hotta, M., Hojo, J., 2009. Effect of AlN additive on densification, microstructure and strength of liquid-phase sintered SiC ceramics by spark plasma sintering. *Journal of the Ceramic Society of Japan*, **117**(1369):1009-1012. [doi:10.2109/jcersj2.117.1009]

Ihle, J., Herrmann, M., Adler, J., 2005a. Phase formation in porous liquid phase sintered silicon carbide: Part I: Interaction between $Al_2O_3$ and SiC. *Journal of the European Ceramic Society*, **25**(7):987-995. [doi:10.1016/j.jeurceramsoc.2004.04.015]

Ihle, J., Herrmann, M., Adler, J., 2005b. Phase formation in porous liquid phase sintered silicon carbide: Part II: Interaction between $Y_2O_3$ and SiC. *Journal of the European Ceramic Society*, **25**(7):997-1003. [doi:10.1016/j.jeurceramsoc.2004.04.016]

Ihle, J., Herrmann, M., Adler, J., 2005c. Phase formation in porous liquid phase sintered silicon carbide: Part III: Interaction between $Al_2O_3$-$Y_2O_3$ and SiC. *Journal of the European Ceramic Society*, **25**(7):1005-1013. [doi:10.1016/j.jeurceramsoc.2004.04.017]

Kim, Y.W., Mitomo, I., Nishimura, T., 2002. High temperature strength of liquid phase sintered SiC with AlN and $Re_2O_3$ (RE=Y, Yb). *Journal of the American Ceramic Society*, **85**(4):1007-1009. [doi:10.1111/j.1151-2916.2002.tb00211.x]

Lee, K.T, Aswath, P.B., 2000. Synthsis of hexacelsian barium aluminosilicate by a solid-state process. *Journal of the American Ceramic Society*, **83**(12):2907-2912. [doi:10.1111/j.1151-2916.2000.tb01659.x]

Lee, K.T, Aswath, P.B., 2001. Enhanced production of celsian barium aluminosilicates by a three-step firing technique. *Materials Chemistry and Physics*, **71**(1):47-52. [doi:10.1016/S0254-0584(00)00525-3]

Lee, S.H., Lee, Y.I., Kim, Y.W., Xie, R.J., Mitomo, M., Zhan, G.D., 2005. Mechanical properties of hot-forged silicon carbide ceramics. *Scripta Materialia*, **52**(2):153-156. [doi:10.1016/j.scriptamat.2004.09.012]

Liu, L.M., Ye, F., Zhang, H.J., Yu, J., Zhang, Z.G., 2009. Celsian formation in $Si_3N_4$-$Ba_{0.75}Sr_{0.25}Si_2Al_2O_8$ composites. *Scripta Materialia*, **60**(6):463-466. [doi:10.1016/j.scriptamat.2008.11.034]

Liu, L.M., Zhou, Y., Zhang, Z.G., 2010. Microstructure compatibility and its effect on the mechanical properties of the α-SiC/β-$Si_3N_4$ co-reinforced barium aluminosilicate glass ceramic matrix composites. *Scripta Materialia*, **63**(2):166-169. [doi:10.1016/j.scriptamat.2010.03.040]

Magnani, G., Brillante, A., Bilotti, I., Beaulardi, L., Trentini, E., 2008. Effects of oxidation on surface stresses and mechanical properties of liquid pressureless-sintered SiC-AlN-$Y_2O_3$ ceramics. *Materials Science and Engineering: A*, **486**(1-2):381-388. [doi:10.1016/j.msea.2007.11.004]

Ortiz, A.L., Cumbrera, F.L., Sánchez-Bajo, F., Guiberteau, F., Xu, H.W., Padture, N.P., 2000. Quantitative phase-composition analysis of liquid-phase-sintered silicon carbide using the rietveld method. *Journal of the American Ceramic Society*, **83**(9):2282-2286. [doi:10.1111/j.1151-2916.2000.tb01548.x]

Rixecker, G., Wiedmann, I., Rosinus, A., Aldinger, F., 2001. *Journal of the European Ceramic Society*, **21**(8):1013-1019. [doi:10.1016/S0955-2219(00)00317-4]

Schwetz, K.A., 2000. Silicon Carbide Based Hard Materials. *In*: Riedel, R. (Ed.), Handbook of Ceramic Hard Materials, Wiley-VCH, Weinheim, p.683-748.

Suzuki, K., Sasaki, M., 2005. Microstructure and mechanical properties of liquid-phase-sintered SiC with AlN and $Y_2O_3$ additions. *Ceramics International*, **31**(5):749-755. [doi:10.1016/j.ceramint.2004.08.014]

Ye, F., Zhou, Y., Lei, T.C., Yang, J.M., Zhang, L.T., 2001. Microstructure and mechanical properties of barium aluminosilicate glass-ceramic matrix composites reinforced with SiC whiskers. *Journal of Materials Science*, **36**(10):2575-2580. [doi:10.1023/A:1017962922590]

Ye, F., Gu, J.C., Zhou, Y., Iwasa, M., 2003. Synthesis of $BaAl_2Si_2O_8$ glass by a sol-gel method and the fabrication of $SiC_{pl}$/$BaAl_2Si_2O_8$ composites. *Journal of the European Ceramic Society*, **23**(13):2203-2209. [doi:10.1016/S0955-2219(03)00042-6]

Ye, F., Liu, L.M., Zhang, J.X., Meng, Q.C., 2008. Synthesis of 30wt%BAS/$Si_3N_4$ composite by spark plasma sintering. *Composites Science and Technology*, **68**(3-4):1073-1079. [doi:10.1016/j.compscitech.2007.07.001]

Ye, F., Liu, L.M., Zhang, H.J., Wen, B.S., 2010. Thermal shock behavior of 30wt% BAS/$Si_3N_4$ self-reinforced composite. *Journal of Alloys and Compounds*, **493**(1-2):272-275. [doi:10.1016/j.jallcom.2009.12.078]

Yu, F., White, K.W., 2001. Relationship between microstructure and mechanical performance of a 70% silicon nitride-30% barium aluminum silicate self-reinforced ceramic composite. *Journal of the American Ceramic Society*, **84**(1):5-12. [doi:10.1111/j.1151-2916.2001.tb00600.x]

Yu, F., Nagarajan, N., Fang, Y., White, K.W., 2001. Microstructural control of a 70% silicon nitride-30% barium aluminum silicate self-reinforced composite. *Journal of the American Ceramic Society*, **84**(1):13-22. [doi:10.1111/j.1151-2916.2001.tb00601.x]

Zhang, J.S., Zhang, Y.Y., Wang, M.T., Xu, F.X., 2007. Microstructure and Properties of Ceramics. Chemical Industry Publishing House, Beijing, China, p.213.

Zhou, Y., Hirao, K., Toriyama, M., Yamauchi, Y., Kanzaki, S., 2001. Effects of intergranular phase chemistry on the microstructure and mechanical properties of silicon carbide ceramics densified with rare-earth oxide and alumina additions. *Journal of the American Ceramic Society*, **84**(7):1642-1644. [doi:10.1111/j.1151-2916.2001.tb00891.x]